

## Steady flow and static stability of airfoils in extreme ground effect

E. O. TUCK

*Applied Mathematics Department, University of Adelaide, Adelaide, S.A. 5001, Australia.*

(Received May 13, 1980)

### SUMMARY

Steady flow over a thin airfoil-like body in close proximity to a plane ground surface is analysed on the basis of a one-dimensional, but non-linear, gap-region flow, matched to the outside via a trailing edge which may possess significant flap-like appendages. The resulting lift and moment predictions are used to estimate quasi-steady stability derivatives in heave and pitch. The results are applied to longitudinal stability of tail-less uncambered airplanes, and to manoeuvring of ships near to a bank, indicating instability in both cases.

### 1. Introduction

In a recent paper [1], an asymptotic theory was developed for unsteady flow induced by an airfoil-like body moving very close to a plane ground surface. The upper and lower surface of the airfoil are both assumed to be close to the ground, their maximum distance from the ground being a factor  $\epsilon \ll 1$  of the airfoil's chord. The thickness/chord ratio and the angle of attack of the airfoil are also small, but may be comparable in magnitude to the clearance ratio  $\epsilon$ .

This theory is an extension of previous work, such as that of Widnall and Barrows [2], who assumed that the thickness/chord ratio and the angle of attack are much smaller than  $\epsilon$ . Such an assumption leads to a linear theory, in which the flow departs little from a uniform stream everywhere. However, if the airfoil's thickness is comparable to its clearance, or (more-importantly) if its angle of attack is comparable to the clearance/chord ratio  $\epsilon$ , the flow in the gap region between airfoil and ground is *not* a small perturbation of the free stream, but may vary by factors of 5 or more from that value, in spite of the fact that the airfoil itself satisfies the usual geometric requirements for linearity.

In the present paper we extend the non-linear theory for steady flow to take account of significant changes in the local angle of attack near the trailing edge. These could arise, for example, from use of a flap or rudder at a high angle of attack, or simply account for a blunt-edged termination.

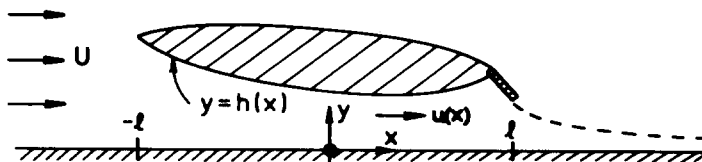


Figure 1. Sketch of steady flow and co-ordinate system.

The essence of the theory is extremely simple. Suppose in the coordinate system of Figure 1 that  $h(x)$  is the local clearance between airfoil and ground at station  $x$ , and  $u(x)$  is the flow velocity in the gap region at that station. Then the one-dimensional character of the flow in the gap demands that  $uh$  is constant. Suppose we write therefore

$$u(x) = \frac{u_0 h_0}{h(x)} \quad (1.1)$$

where  $h_0$  is the trailing-edge clearance and  $u_0$  the (unknown) speed at which the gap flow emerges at the trailing edge. Our primary task is to determine  $u_0$ , by matching with the flow above the airfoil.

But, because the whole airfoil is thin, with a maximum relative departure from the ground of  $O(\epsilon)$ , the flow is a small  $O(\epsilon)$  perturbation to the uniform stream  $U$ , everywhere except in the gap region. Hence the pressure in the flow departs from the ambient level only by a small  $O(\epsilon)$  quantity, except in the gap. This has two important consequences.

One immediate consequence is that as soon as the unknown trailing-edge velocity  $u_0$  is determined, the lift (and moment) on the airfoil is also determined with relative error  $O(\epsilon)$ , by the so-determined non-trivial under-body flow (1.1).

Specifically, if  $p$  denotes the excess of pressure over the free-stream value, the Bernoulli equation states that

$$\frac{p}{\rho} + \frac{1}{2} q^2 = \frac{1}{2} U^2 \quad (1.2)$$

everywhere in the flow, where  $q$  is the fluid velocity magnitude. But since  $q = U + O(\epsilon)$  on the upper surface of the airfoil but  $q - U = O(1)$  on the lower surface, the net lift force is obtained to leading order by integrating just the *lower* surface pressure

$$p(x) = \frac{1}{2} \rho U^2 \left[ 1 - \sigma^2 \frac{h_0^2}{h^2(x)} \right] + O(\epsilon), \quad (1.3)$$

where

$$\sigma = u_0/U \quad (1.4)$$

is the ratio between trailing-edge and free-stream speeds.

In fact, as shown formally in [1],  $\sigma = 1$  or  $u_0 = U$ , unless there is a flap-like trailing-edge appendage. This is almost obvious, since if one pursues further the argument above, concerning the small departure of the above-airfoil flow from the uniform stream, there seems little choice but to demand that the emerging gap flow  $u_0$  at the trailing edge agree with this value  $U$ . However, the nature of this matching process is a little more subtle, and depends on the properties of the vortex sheet that springs from the trailing edge.

This matching is discussed further in Sec. 2, and extended to the case when there is a trailing-edge appendage. The conclusion is that the parameter  $\sigma$  can then be obtained by solving a classical free-streamline problem. This problem is identical to that for a jet produced by an effective nozzle or mouthpiece, formed between the appendage and the ground plane, and  $\sigma$  is the contraction coefficient of that nozzle.

As an illustration of the procedure for determining the contraction coefficient  $\sigma$ , in Sec. 3 we give the solution for a simple hinged flap, using conformal mapping in the hodograph plane. The output is a plot of  $\sigma$  as a function of the flap angle and size, relative to the trailing-edge gap. Once such a computation is performed for any given appendage geometry, the exact details of this geometry can subsequently be ignored, since the only influence on the airfoil as a whole occurs via the parameter  $\sigma$ , as in (1.3).

In Sec. 4, we complete the steady solution, by integrating the pressure (1.3) to give the lift force and pitching moment on the airfoil. The special case of a flat under surface, in which  $h'(x)$  is constant, is treated in detail.

These results are then used in Sec. 5 to study stability of an airfoil close to the ground and of a ship in shallow water close to a lateral plane boundary. In the former case a flat tail-less under surface appears to be generally unstable. In the latter case, the equilibrium configuration with non-zero fixed rudder angle is always unstable.

## 2. Trailing-edge matching

The local flow in the neighbourhood of the trailing edge is illustrated in Figure 2. The scale of this figure is everywhere  $O(\epsilon\ell)$ . That is, we are only concerned with horizontal and vertical distances from the trailing edge that are comparable with the local clearance, and hence small compared to the airfoil's chord  $2\ell$ .

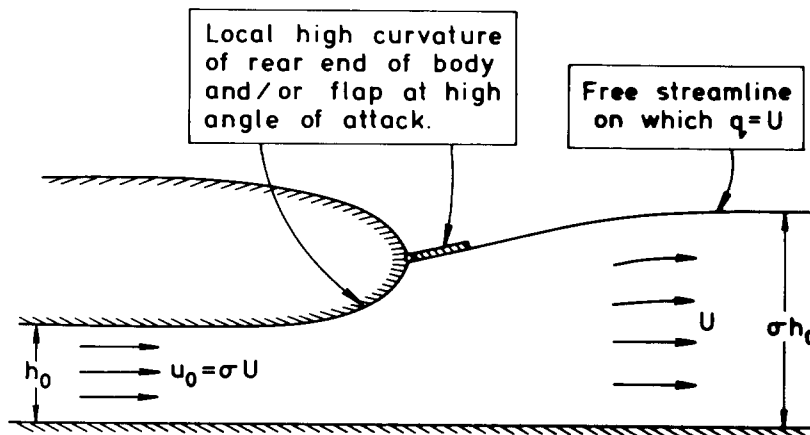


Figure 2. Local flow near trailing edge, for an example like the stern of a ship with a rudder.

The gap-region 'trailing-edge clearance'  $h_0$  as defined in equation (1.1) is now interpreted as the apparent clearance in the limiting uniform-gap region at  $x = -\infty$ , of this local region. In this uniform channel, we assume an approaching uniform stream of magnitude  $u_0$ , modelling the gap-region's trailing-edge velocity. As this entering uniform flow encounters changes in the geometry of the channel, its magnitude changes, until eventually it must arrive at  $x = +\infty$  with the free-stream velocity  $U$ .

Certainly if there are *no such* changes in geometry, the flow remains uniform and we must have  $u_0 = U$ . In this case, the vortex sheet that springs from the actual trailing edge is the plane surface  $y = h_0$ , across which neither velocity nor pressure is discontinuous, since both take free-stream values, to within an  $O(\epsilon)$  error. This situation occurs when all lower surfaces of the airfoil, including the flap, if any, are at small angles to the horizontal. Formally, providing all such angles tend to zero as  $\epsilon \rightarrow 0$ , the limiting geometry has only horizontal boundaries. This case was studied in [1].

The only possibility in which a non-trivial trailing-edge flow occurs, is that in which some surfaces are at finite angles to the horizontal. Naturally, this cannot happen over any significant distance, since if it did, either the airfoil would make contact with the ground, or else the idea that the whole airfoil is a small perturber of the uniform stream would break down. However, nothing prevents a finite angle of attack for facets of the body's surface that extend only over distances of  $O(\epsilon\ell)$ , such as are represented by the scale of the local flow at the trailing edge.

Now, when such a situation occurs, the vortex sheet springing from the trailing edge is no longer plane, but lies in a non-trivial continuous surface whose shape must be determined. The condition that determines this shape is continuity of pressure across the surface, which, for steady flow, is equivalent to continuity of velocity magnitude. But, with error  $O(\epsilon)$ , the velocity magnitude in the flow *above* the vortex sheet is equal to the free-stream speed  $U$ . Hence, the boundary condition determining the shape of the streamline representing the vortex sheet is  $q = U$ .

We are now able to recognise the problem of Figure 2 as a classical free-streamline problem, c.f. Gilbarg [3]. That is, the original uniform stream  $u_0$  emerges from its constant-width channel at  $x = -\infty$ , separates from the trailing edge, and continues as a free jet, confined between the ground surface  $y = 0$ , and the free surface on which  $q = U$ . Eventually, as  $x \rightarrow +\infty$ , this jet will settle down to a uniform stream with the free-stream velocity  $U$ , and at a constant width that must equal  $h_0 u_0 / U$  by continuity.

The quantity  $\sigma$  introduced in equation (1.4) is now also recognisable as the 'contraction coefficient' of this jet, i.e. as the ratio between the jet's width at  $x = +\infty$ , and the channel width at  $x = -\infty$ . If the local-flow problem is appropriately scaled (e.g. by choosing  $h_0$  as a fundamental length, and  $U$  as a fundamental velocity), it is clear that the quantity  $\sigma$  is a non-dimensional output from the scaled problem, dependent only on the relative geometry of the effective geometry of the effective 'nozzle' formed by the trailing edge or flap. It is only through the quantity  $\sigma$  that this geometry influences the net force distribution on the airfoil, and hence we may concentrate our efforts on its determination; subsequently we may ignore the trailing-edge geometry entirely. As an example, in the following section we use classical hodograph techniques to determine  $\sigma$  for a special flap-like geometry.

### 3. Contraction coefficient for a flap

The two-dimensional nozzle problem depicted in Figure 3, consists simply of a uniform unit-width channel in  $x < 0$ , with a flap of length  $\beta$ , attached in  $x > 0$  at angle  $\alpha$  to the horizontal. The non-dimensional entering flow has magnitude  $\sigma$  at  $x = -\infty$ , and the resulting unit-velocity jet at  $x = +\infty$  has width  $\sigma$ . The jet is an expansion if  $\alpha > 0$  and  $\sigma > 1$  as sketched, but a contraction if  $\alpha < 0$ ,  $\sigma < 1$ .

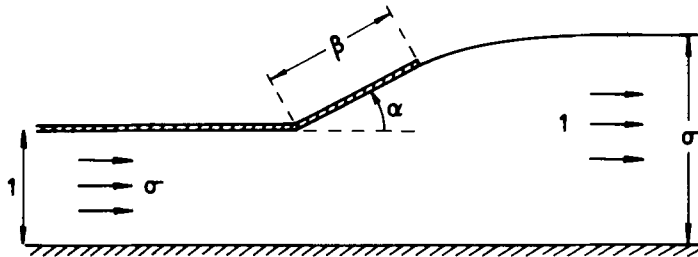


Figure 3. Special trailing-edge local flow, for a flat plate with a hinged plane flap.

Although this is a classical hodograph problem that has been solved by a number of previous authors (e.g. see Gurevich, [4], p. 57), the results do not seem to have been cast in the form needed here, namely as output values of  $\sigma = \sigma(\alpha, \beta)$ , and hence we repeat the solution for completeness. If  $f = \phi + i\psi$  is the complex potential, and  $\Omega = \log f'(z)$ , where  $z = x + iy$ , the problem is solved by the mapping

$$\cosh \left( \frac{\pi}{\alpha} \Omega \right) = \frac{e^{\pi f/\sigma} + \lambda}{e^{\pi f/\sigma} + 1} \tag{3.1}$$

between the  $f$  and  $\Omega$  planes illustrated in Figure 4, where

$$\lambda = \cosh \left( \frac{\pi}{\alpha} \log \sigma \right). \tag{3.2}$$

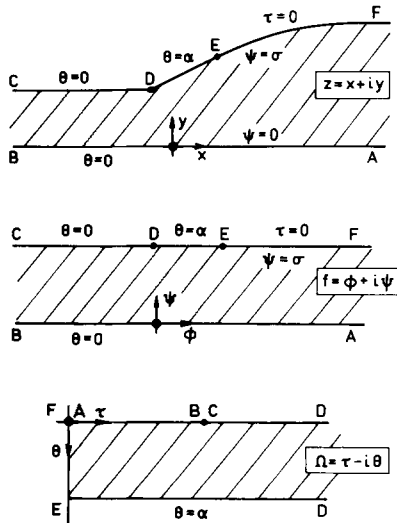


Figure 4. Conformal mapping to solve problem of Figure 3.

The flow in the physical  $z$ -plane is recovered from this mapping by integrating

$$\frac{dz}{d\Omega} = -\frac{\sigma}{\alpha} (\lambda-1) \frac{e^{-\Omega} \sinh \frac{\pi\Omega}{\alpha}}{\left(\cosh \frac{\pi\Omega}{\alpha} - 1\right) \left(\lambda - \cosh \frac{\pi\Omega}{\alpha}\right)} \quad (3.3)$$

over appropriate contours. In particular, if we integrate over DE, we obtain the flap length as

$$\beta = \frac{\sigma}{\alpha} (\lambda-1) \int_0^\infty \frac{e^{-\Omega} \sinh \frac{\pi\Omega}{\alpha} d\Omega}{\left(\cosh \frac{\pi\Omega}{\alpha} + 1\right) \left(\lambda + \cosh \frac{\pi\Omega}{\alpha}\right)} \quad (3.4)$$

for  $\alpha > 0$ . If  $\alpha < 0$ , the factor  $e^{-\Omega}$  in (3.4) is replaced by  $e^{\Omega}$ . This formula (3.4) agrees (after some manipulation) with Gurevich's ([4], p. 72) equation (2.30).

Thus (3.4) enables computation of  $\beta = \beta(\alpha, \sigma)$  from which, by cross-plotting, we are able to recover  $\sigma = \sigma(\alpha, \beta)$ . Results computed using the trapezoidal rule on a TRS-80 micro-computer are given in Figure 5. Note that if  $\beta < 1$ , the flap may be allowed to extend backwards, i.e. have  $\alpha < -\pi/2$ , and  $\sigma$  takes its minimum value for  $\alpha$  values slightly less than  $-\pi/2$ . If  $\beta > 1$ , the flap contacts the ground at an  $\alpha$  value greater than  $-\pi/2$ , at which point we must have  $\sigma = 0$ . The flow is unlikely to be realistic for large *positive* values of flap angle since separation will occur in practice before the trailing edge is reached; however, in principle the mathematical solution is valid up to  $\alpha = +\pi$ , and suggests  $\sigma \rightarrow \infty$  as  $\alpha \rightarrow +\pi$ .

The range of greatest interest is that for quite small flap angles  $\alpha$ , where the behaviour of  $\sigma$  as a function of  $\alpha$  is approximately linear. The slope of this linear dependence is also nearly a linearly increasing function of the flap length  $\beta$  for small values of  $\beta$ . However, beyond  $\beta = 0.5$  (i.e. a flap that is capable of blocking half of the trailing-edge clearance) there is a diminished effectiveness of further increases in flap length.

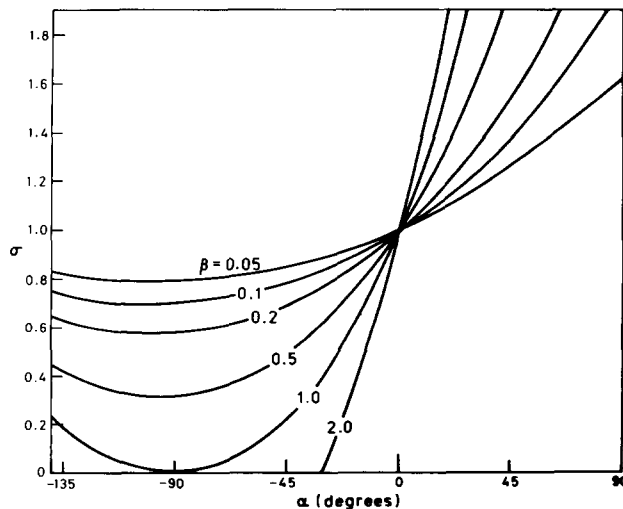


Figure 5. Computed contraction coefficient for the problem of Figure 3.

#### 4. Lift, moment and centre of pressure

Upon integration of the pressure given by (1.3) over the chord  $2\ell$ , from  $x = -\ell$  to  $x = \ell$ , we find the resultant (away-from-ground) lift force,

$$L = \rho U^2 \ell [1 - \sigma^2 \lambda], \quad (4.1)$$

and moment (leading edge up) about the mid-chord point  $x = 0$ ,

$$M_0 = \rho U^2 \ell^2 \sigma^2 \mu, \quad (4.2)$$

where

$$\lambda = \frac{1}{2\ell} \int_{-\ell}^{\ell} \left[ \frac{h_0}{h(x)} \right]^2 dx \quad (4.3)$$

and

$$\mu = \frac{1}{2\ell^2} \int_{-\ell}^{\ell} x \left[ \frac{h_0}{h(x)} \right]^2 dx \quad (4.4)$$

are non-dimensional parameters categorizing the mean inverse-square clearance and its moment, respectively.

In circumstances under which the clearance  $h(x)$  is almost uniform, i.e.

$$h(x) = h_0 + h_1(x) \quad (4.5)$$

where  $h_1(x) \ll h_0$ , we can linearize the above results to give

$$\lambda = 1 - \frac{1}{h_0 \ell} \int_{-\ell}^{\ell} h_1(x) dx \quad (4.6)$$

and

$$\mu = -\frac{1}{h_0 \ell^2} \int_{-\ell}^{\ell} x h_1(x) dx. \quad (4.7)$$

If, at the same time, we set  $\sigma = 1$ , i.e. there are no stern appendages, the lift becomes simply

$$L = \frac{\rho U^2}{h_0} \int_{-\ell}^{\ell} h_1(x) dx \quad (4.8)$$

and the moment about the origin is

$$M_0 = -\frac{\rho U^2}{h_0} \int_{-\ell}^{\ell} x h_1(x) dx. \quad (4.9)$$

In this linearized case, equivalent to the theory of Widnall and Barrows [2], the lift and moment are both inversely proportional to the trailing-edge clearance  $h_0$ . The lift is also proportional to the area lying between the under surface of the body and a horizontal line drawn through its trailing edge, and the moment is such that the centre of pressure lies at the centre of that area. The inverse proportionality on clearance indicates clearly the profound influence of the ground when the clearance is very small, but clearly this linearization must break down when  $h_0$  is small enough for variations in clearance along the chord to be comparable to the trailing-edge clearance itself, in which case we must revert to the full formulae (4.3), (4.4).

As a test of the full non-linear theory, suppose that the under surface of the body in the main gap region consists of a plane surface at angle of attack  $\theta$  to the free stream, i.e.

$$h(x) = h_0 + \theta(\ell - x), \quad (4.10)$$

then

$$\lambda = \frac{h_0}{h_0 + 2\ell\theta} = \frac{h(\ell)}{h(-\ell)} \quad (4.11)$$

and

$$\mu = \lambda \left( \frac{1+\lambda}{1-\lambda} \right) + 2 \left( \frac{\lambda}{1-\lambda} \right)^2 \log \lambda. \quad (4.12)$$

Thus, in this case,  $\lambda$  is simply the ratio between trailing and leading-edge clearance, and  $\mu$  is a definite function of  $\lambda$ .

In order to plot variation of  $L$  and  $M_0$  with angle of attack  $\theta$  let us suppose for the present section that we fix the *mean* clearance  $h(0) = h_0 + \theta\ell$ . Then both  $\lambda$  and  $\mu$  can be considered functions of the normalized angle of attack

$$\bar{\theta} = \theta \left( \frac{\ell}{h(0)} \right) = \frac{1-\lambda}{1+\lambda} \quad (4.13)$$

and so is therefore the lift coefficient

$$C_L = \frac{L}{\rho U^2 \ell} \quad (4.14)$$

and centre of pressure location

$$x_p = - \frac{M_0}{L}. \quad (4.15)$$

The quantity  $\bar{\theta}$  takes values between  $\bar{\theta} = +1$  when the trailing edge hits the ground, and  $\bar{\theta} = -1$ , when the leading edge hits the ground. Figures 6, 7 show plots of  $C_L(\bar{\theta})$  and  $x_p(\bar{\theta})/\ell$  respectively, for various values of the contraction coefficient  $\sigma$ .

The case  $\sigma = 1$  corresponds to absence of trailing-edge appendages, and is of the greatest importance. In that case  $C_L(0) = 0$ , i.e. the lift vanishes, as expected, at zero angle of attack. The linear theory, as in (4.8), (4.9), corresponds to small values of  $\bar{\theta}$ , with  $\theta \ll h(0)/\ell$ . However, the present theory is specifically valid for  $O(1)$  values of the *normalized* angle of attack  $\bar{\theta}$ , i.e.



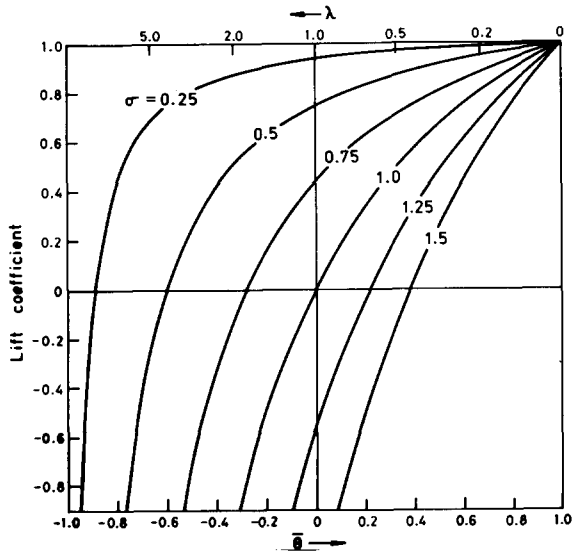


Figure 6. Lift coefficient for an airfoil with a plane lower surface at an angle of attack  $\theta$ , plotted against  $\bar{\theta} = \theta c/h(0)$ , where  $2c$  is the chord and  $h(0)$  the clearance to the ground at mid-chord, for various values of the trailing-edge contraction coefficient  $\sigma$ .

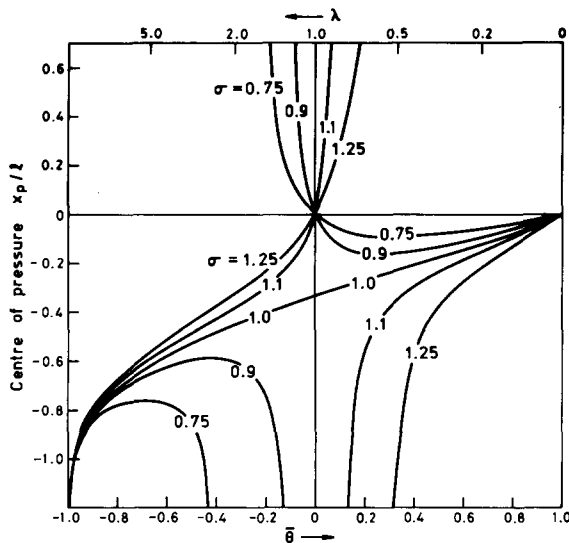


Figure 7. Location  $x = x_p$  of the centre of pressure at which the lift in Figure 6 acts.

for actual angles of attack  $\theta$  comparable to  $h(0)/\ell$ , for which  $C_L = O(1)$ . This again exemplifies the profound effect of the ground surface on the lift, since, in the absence of ground effect, the lift is a small  $O(\epsilon)$  quantity, whenever the true angle of attack  $\theta$  is  $O(\epsilon)$ .

The maximum positive lift coefficient is *unity*, attained for all  $\sigma$  when  $\bar{\theta} = 1$ , i.e. when the trailing edge of the foil just makes contact with the ground, so stalling the gap flow and subjecting the complete underside of the foil to the full uniform stagnation pressure. Such a result also applies for all  $\theta$  if  $\sigma = 0$ , of course, since again this corresponds to a stern appendage that just contacts the ground surface.

Conversely, the lift tends to minus infinity for all  $\sigma$ , when  $\bar{\theta} \rightarrow -1$ . That is, as the leading edge approaches the ground, the velocity with which the fluid must pass through this vanishingly-small gap at the leading edge tends to infinity, and the resulting low pressure sucks the foil downward by a greater and greater amount.

The centre of pressure shown in Figure 7 lies at the 1/3-chord point  $x = -\ell/3$ , when  $\sigma = 1$  and  $\bar{\theta}$  is small. This is the natural consequence of the linear theory, since the area whose centroid defines the centre of pressure is now a triangle with apex at the trailing edge.

However, this particular centre-of-pressure conclusion is highly sensitive to the contraction coefficient  $\sigma$ , and hence to the setting of any trailing-edge flap or rudder. In particular, for all  $\sigma$  values other than unity, the centre of pressure is at *mid-chord* for small angles of attack. For  $\sigma < 1$ , e.g. for a flap angled toward the wall, and thus augmenting the lift due to angle of attack, the centre of pressure then moves *forward* as the angle of attack increases, and reaches a maximum forward location that is necessarily aft of the 1/3-chord point, before moving back toward the mid-chord position as  $\bar{\theta} \rightarrow 1$ .

If  $\sigma > 1$ , e.g. for a flap angled away from the wall, the centre of pressure is located in the rear half of the body, for those small positive angles of attack such that the flap keeps the net lift negative. As soon as the angle of attack is high enough to overcome the effect of the flap, and create a net positive lift, the centre of pressure shifts ahead of the body. Further increases in angle of attack shift the centre of pressure aft, and again it approaches mid-chord as  $\bar{\theta} \rightarrow 1$ .

These results indicate rather dramatic variations of lift and centre of pressure location, as we vary either the angle of attack of the airfoil as a whole, or the flap angle. It should, however, be recalled that Figures 6, 7 are plots for fixed values of the mean clearance ratio  $h(0)/\ell$ , and hence their dynamic significance is not entirely clear. In any actual manoeuvre of a wing-like body near a plane surface, it is to be expected that the mean clearance will vary significantly. Some guidance for dynamic analysis of such manoeuvres is provided in the following section.

## 5. Stability of coupled heave and pitch

In the absence of ground effect, a thin airfoil is essentially neutrally or marginally stable in heave, one altitude being indistinguishable from any other. An uncambered thin airfoil alone in an infinite fluid is also neutral in pitch, since the centre of pressure is then invariant with angle of attack. Normal positive camber (concave downwards) leads to instability of the bare airfoil, which then conventionally requires a subsidiary small lifting surface, such as a tail, to restore stability. These static-stability considerations are amplified in standard aeronautical texts such as that of Irving [5], the important simplifying feature being that the pitching mode can be treated without any form of coupling to other modes.

The situation for an airfoil in extreme ground effect is markedly different. In the first place, heave is no longer a neutral mode, but is strongly stabilised by the ground effect. Any increase in altitude (at fixed angle of attack) reduces the lift, so causing a return to the original altitude.

The question of stability in pitch at fixed (mean) height can be answered by reference to results such as those in Figure 7. For a flat under-surface, this figure indicates stability for those portions of the curves with positive slope as a function of angle of attack. Thus, whenever an increase in angle of attack at fixed mean height shifts the centre of pressure *rearward*, there is a net restoring moment, and the situation is stable.

Unfortunately, pitch need not occur at fixed mean height, and it is necessary to treat the full coupled heave and pitch motions. We do this here in a quasi-steady manner. That is, we assume that the lift  $L$  and moment  $M_0$  are given by (4.1) and (4.2) at all times. This neglects all unsteady-flow effects such as vortex shedding, and can be expected to provide a good approximation for sufficiently slow perturbations. In view of the fact that we have in this way neglected the only possible dissipation mechanism in the (inviscid) problem, we cannot expect damping of any oscillations.

In the present section, we use 'h' for the height  $h(x_g)$  of the centre of gravity  $x = x_g$ , with  $\theta$  as before the angle of attack. Then we consider  $L = L(h, \theta)$  and  $M_0 = M_0(h, \theta)$  to be known functions, but work also with the moment

$$M = M_0 + x_g L \quad (5.1)$$

about the centre of gravity. If there are any subsidiary lifting surfaces, i.e. tails, etc., their effect is assumed to be included with  $L$  and  $M$ , which represent the total lift and moment for a vehicle.

Now if  $m$  is the mass and  $k$  the radius of gyration of the mass about the centre of gravity, the equations of motion are

$$m \frac{d^2 h}{dt^2} = L(h, \theta) - mg \quad (5.2)$$

and

$$mk^2 \frac{d^2 \theta}{dt^2} = M(h, \theta). \quad (5.3)$$

Any equilibrium state  $h = \bar{h}$ ,  $\theta = \bar{\theta}$  must have  $L = mg$  (i.e. the lift supports the weight) and  $M = 0$ , i.e.

$$x_g = x_p = -M_0/L, \quad (5.4)$$

with the centre of gravity coincident with the centre of pressure.

Small perturbations  $h = \bar{h} + \delta h$ ,  $\theta = \bar{\theta} + \delta \theta$  about such an equilibrium state satisfy

$$m \frac{d^2}{dt^2} \delta h = L_h \delta h + L_\theta \delta \theta \quad (5.5)$$

and

$$mk^2 \frac{d^2}{dt^2} \delta\theta = M_h \delta h + M_\theta \delta\theta, \quad (5.6)$$

subscripts denoting partial derivatives evaluated at the equilibrium point.

The linear pair of constant-coefficient equations (5.5), (5.6) can be analysed completely for stability. The solution consists of bounded oscillations, and can be described as *stable*, if the following *strict* inequalities hold:

$$\Delta^2 = L_h M_\theta - L_\theta M_h > 0 \quad (5.7)$$

and

$$M_\theta + k^2 L_h < -2k\Delta. \quad (5.8)$$

If *either* of the inequalities (5.7), (5.8) is reversed, the motion contains oscillations whose amplitude grows exponentially with time, and the situation can be described as unstable.

Marginal states in which one or both of the inequalities (5.7), (5.8) become equalities could be described as neutrally stable, but in practice are effectively unstable, since they correspond to a drift away from equilibrium. In particular, if (5.8) becomes an equality, the amplitude of the oscillations builds up at a linear rate with time, rather than the exponential rate for true stability. If (5.7) becomes an equality, bounded oscillations occur about a mean level that may drift at a constant rate (constant vertical velocity and/or constant pitch angular velocity). Finally if *both* (5.7) and (5.8) become equalities, there are no oscillations, but both displacements drift at a constant rate.

For example, in the absence of ground effect, neither  $L$  nor  $M$  depends on  $h$  and (5.7) becomes an equality, while (5.8) reduces to

$$M_\theta < 0. \quad (5.9)$$

This is the classical pitch stability condition for airplanes [5]. Note that in this case pitch is decoupled from heave, and in the stable case when (5.9) is satisfied, only the vertical motion is subject to a constant speed drift. If we restrict further to a tail-less un-cambered airfoil, the equilibrium condition  $M = 0$  implies  $M_\theta = 0$ , so that (5.9) also becomes an equality, and the angle of attack also drifts at a constant rate.

Note that the left-hand side of (5.8) incorporates the two restoring terms from the equations of motion (5.5), (5.6). Thus a negative value for  $L_h$  and a negative value for  $M_\theta$  indicates separate stability in uncoupled heave and pitch respectively. The corresponding coupled motion is stable only if an appropriately weighted sum of these coefficients is *sufficiently* negative, and at the same time (5.7) is satisfied.

This inequality (5.7) demands that the heave-pitch coupling be not too vigorous. This condition can be simplified, since terms arising from the change to a centre-of-gravity system do not contribute. Thus

$$\Delta^2 = \partial(L, M)/\partial(h, \theta) = \partial(L, M_0)/\partial(h, \theta) = \partial(L, M_0)/\partial(h_1, \theta) \quad (5.10)$$

$$= -(\rho U^2 \sigma^2)^2 \ell^3 \partial(\lambda, \mu)/\partial(h_1, \theta) \quad (5.11)$$

where  $h_1$  is any value of  $h(x)$ . Equation (5.11) assumes that the complete lift and moment are given by (4.1), (4.2) i.e. that the subsidiary control surfaces, if any, are also in ground effect, and are lumped together with the main airfoil in the over-all clearance function  $h(x)$ . Note that in this case, the stability condition (5.7) reduces to

$$\partial(\lambda, \mu)/\partial(h_1, \theta) < 0 \quad (5.12)$$

and is independent of trailing appendage effects, that enter via the contraction coefficient  $\sigma$ .

For example, if the lower surface of the airfoil is plane, with  $h(x)$  given by (4.10),  $\mu = \mu(\lambda)$  and (5.12) becomes an equality. Thus, as far as this stability criterion is concerned, such a ground-effect airfoil is neutrally stable. The remaining stability criterion (5.8) now reduces to (5.9), which requires that

$$\frac{x_p}{\ell} < \frac{d\mu}{d\lambda} \quad (5.13)$$

and is satisfied at positive lift if

$$\frac{dx_p}{d\lambda} < 0 \quad (5.14)$$

or (referring to Figure 7)  $dx_p/d\bar{\theta} > 0$ .

Thus, those portions of the curve of Figure 7 with negative slope are definitely unstable. Those portions with positive slope are (in principle) neutrally stable. However, unlike the corresponding situation in the absence of ground effect, the fact that there is now coupling between heave and pitch means that a constant-speed drift occurs with respect to *both* modes, and the situation is, in effect, unstable.

An alternative viewpoint on such marginal states is that any drift must be between equilibrium states. For a stable airfoil in the absence of ground effect, such a drift occurs only with respect to the heave mode, since equilibrium is possible at fixed angle of attack for all altitudes. However, in the present case, if equilibrium is to be maintained, and there is an increase in altitude, the angle of attack must increase, to compensate for the decrease in lift that would otherwise occur. Thus 'neutral stability' now involves changes *both* in altitude and angle of attack, and is thus less tolerable.

Further discussion of the longitudinal stability problem for ground-effect vehicles would require analysis of the effect of camber, and of tail surfaces, and is beyond the scope of the present paper. Another application for which stability questions arise is, however, that for ships moving in shallow water close to a side-wall or canal bank. This is simply the case  $g = 0$  of the present analysis, i.e. gravity no longer provides a 'heave' restoring force toward the wall. If the clearance between the bottom of the ship and the bottom of the water is small, a two-dimensional theory can be used in the horizontal plane ([6], [7]).

For  $g = 0$ , equilibrium demands both  $L = 0$  and  $M = 0$ . Thus we must have

$$\lambda = \sigma^{-2} \quad (5.15)$$

and

$$\mu = 0. \quad (5.16)$$

This is certainly possible with  $\sigma = 1$  (i.e. without rudder) for a flat surface  $h(x) = h_0$  at zero angle of attack. However, this is hardly a useful conclusion for realistic ships, whose surface nearest to the wall will always be curved, indeed cambered toward the wall. For example, suppose the ship possesses fore-and-aft symmetry, and is at zero angle of attack, with  $h(x) = h_0 - \frac{1}{2}B(x)$ ,  $B(x)$  being the beam. Then  $\mu = 0$  by symmetry, and the rudder must be set at an angle such that  $\sigma = \lambda^{-\frac{1}{2}} < 1$ .

We now question the stability of such a configuration with  $\sigma$  fixed, by setting

$$h(x) = h_0 - \frac{1}{2}B(x) + \theta(\ell - x), \quad (5.17)$$

performing the required differentiations, and then letting  $\theta \rightarrow 0$ . The coupling condition (5.12) is seen to be satisfied, but both  $M_\theta > 0$  and  $L_h > 0$  in this case, so that there is no possibility of satisfying (5.8). Thus a ship cannot move parallel and very close to a plane side wall without dynamic rudder control. This agrees with the conclusions of Hess [8], who used a linear theory for not-so-small distances from the wall.

#### REFERENCES

- [1] E. O. Tuck, A non-linear unsteady one-dimensional theory for wings in extreme ground effect, *J. Fluid Mech.* 98 (1980) 33-47.
- [2] S. E. Widnall and T. M. Barrows, An analytic solution for two- and three-dimensional wings in ground effect, *J. Fluid Mech.* 41 (1970) 769-792.
- [3] D. Gilbarg, *Jets and cavities*, in Handbuch der Physik (ed. Flugge, S.), Vol. IX (1960) 311-438.
- [4] M. I. Gurevich, *Theory of jets in ideal fluids*, Academic Press, New York, 1965.
- [5] F. G. Irving, *An introduction to the longitudinal static stability of low-speed aircraft*, Pergamon, Oxford, 1966.
- [6] E. O. Tuck, Hydrodynamic problems of ships in restricted waters, *Ann. Rev. Fluid Mech.* 10 (1978) 33-46.
- [7] F. Hess, Rudder effectiveness and course-keeping stability in shallow water: a theoretical model, *International Shipbuilding Progress* 24 (1977) 206-221.
- [8] F. Hess, Ships in shallow canals: a theoretical model for lateral forces, rudder effectiveness and course-keeping stability, *International Shipbuilding Progress* 26 (1979) 233-240.